PEER-REVIEWED ARTICLE

PRACTICAL PAPER

Applications of the IHS Color Transformation for 1:24,000-Scale Geologic Mapping: A Low Cost SPOT Alternative

Abstract

The spatial resolution of multispectral satellite imagery can be greatly improved through the application of the IHS color transformation. This numerical transformation allows diverse forms of data from space- and air-borne platforms to be combined into a single hybrid data set. Procedures are given for merging readily available Landsat MSS bands with digitized aerial photographs to produce color imagery having SPOT-like spectral (green to near-infrared) and spatial (10-m) properties. Geomorphic interpretation is improved because both sources of information are available for large-scale spectral discrimination of surface materials and spatial analysis of associated landforms.

Two alternative methods, both using only the reverse IHS transformation, are also presented for combining spectrally dissimilar data. These methods enhance geologic discrimination by allowing short-wave infrared data to be used in conjunction with the spatial information content of an aerial photograph. Spectral image maps that depict the mineralogy of geologic surface materials in progressively changing colors can be prepared and integrated, for example, as thematic overlays for high-resolution photographic base images. These "colorized" images improve terrain interpretation and mapping by revealing critical geologic relationships between the lithologic composition of surface materials and associated landform morphology.

Introduction

Earth scientists commonly use aerial photographs to map landforms on the basis of their morphology, pattern, texture, and spatial association to other photographically identifiable landscape features (Avery and Berlin, 1985). While these methods have proven adequate, advancements in multispectral satellite coverage and computer technologies for integrating diverse forms of digital and analog terrain data provide a greater assortment of remote sensing tools.

The broad spectral coverage of modern satellite sensors, such as Landsat, extends our view of the Earth well beyond the visible capabilities of human perception into the geologically important short-wave and thermal infrared regions of the electromagnetic spectrum. These multi-band data enable surface sediment composition and soil patterns to be interpreted and their geologic relationships to be revealed through the application of well established digital enhancement and analysis techniques including band ratioing, density slicing, principal components analysis, and multispectral classification (Drury, 1987; Jensen, 1986; Lang *et al.*, 1984a, 1984b; Shih and Schowengerdt, 1983; Rowan *et al.*, 1983; Goetz and Rowan, 1981; Segal and Gillespie, 1980; Moik, 1980; Kahle, *1980a, 1980b*).

A notable limitation of Landsat is its relatively poor spatial resolution for large-scale (1:24,000) geologic analysis and mapping of small landforms. The digital (raster) format of these data does, however, provide a means for integrating higher resolution information from such sources as aerial photographs, space- and air-borne radar images, and large-scale thematic maps. The merger of readily available NASA or NHAP aerial photographs with multi-band Landsat data, for instance, permits the topographic (spatial) resolving power of the photograph to be used in conjunction with the geologic (spectral) discrimination capabilities of Landsat.

Combining High- and Low-Resolution Image Data

Previous Approaches

Several methods have been devised to combine remotely sensed data. Common pixel-by-pixel mathematical procedures including adding, subtracting, and ratioing have been successfully used to merge Landsat spectral bands with digitized aerial photographs (Chavez, 1986) and 10-m SPOT (Systeme Pour l'Observation de la Terre) panchromatic data (Chavez and Bowell, 1988). Other, more complex procedures, such as selective principal components and band replacement (an image compilation method using a co-registered digitized aerial photograph in place of a Landsat image band for the red-green-blue color display), have also been employed to improve the resolution of multi-band satellite images (Chavez, 1986; Cliche *et al.*, 1985; Chavez *et al.*, 1982, 1984).

While these procedures may offer improvements in spatial resolution, the ensuing images often exhibit residual noise, when input bands are highly correlated, or colors that are difficult to explain; the latter being a distinct disadvantage of selective principal components merging. Additionally, the merger may be limited to imagery having similar spatial (pixel size) traits. Chavez (1986) noted for instance that band replacement is best applied to data with small (2× to 3×) differences in spatial resolution. Another problem is that the method used to combine the data sets may adversely

*Dennis N. Grasso**
Department of Geology and Geophysics, University of Wyoming, Laramie, WY 82070
*Presently with the Water Resources Division, U. S. Geological Survey, 6770 South Paradise Road, Las Vegas, NV 89119

Photogrammetric Engineering & Remote Sensing, Vol. 59, No. 1, January 1993, pp. 73–80.

0099-1112/93/5901–69$03.00/0

alter the information content of the resulting image product (Chavez and Bowell, 1988). Such an alteration might create a particularly undesirable situation if the original multi-band data set is needed for subsequent spectral analysis.

IHS Transformation Merger

A digital color enhancement technique that has recently received noteworthy attention as an image merging tool is the IHS (intensity-hue-saturation) transformation. This numerical procedure was developed to convert a three-band RGB (red-green-blue) display into its fundamental physiological (IHS) elements of human color perception (Buchanan and Pendergrass, 1980). Various IHS transformation algorithms and their remote sensing applications have been reported on by Judd and Wyszecki (1975), Gillespie (1980), Haydn *et al.* (1982), Daily (1983), King *et al.* (1984), Gillespie *et al.* (1986), Lillesand and Kiefer (1987), Robertson and O'Callaghan (1988), Carper *et al.* (1990), and Harris *et al.* (1990). All are based on the tristimulus theory of color (Gillespie, 1980), and differ principally in their method for deriving intensity (Carper *et al.*, 1990).

Two notable virtues of the IHS transformation are (1) its ability to effectively separate spatial (intensity) and spectral (hue and saturation) information from a standard RGB image, and (2) its ability to convert IHS elements back to RGB display components. The forward (RGB to IHS) transformation produces intensity images that contain average brightness (spatial) information (Gillespie, 1980) corresponding to surface roughness or morphology, and hue and saturation images that contain color (spectral) information related to surface reflectivity or composition. If the intensity image is enhanced using an edge-enhancement or high-boost filter, or replaced with an image having higher spatial resolution, the reverse (IHS to RGB) transformation will produce RGB output images having similarly enhanced spatial resolution and color (hue and saturation) comparable to the original RGB input bands. The IHS transformation can, therefore, be used as an image merging tool to integrate spatial and spectral data by allowing a co-registered, high-resolution image (e.g., a digitized aerial photograph) to be used in place of the intensity component prior to performing the reverse transformation.

This technique has been used to merge SPOT 20-m multispectral (XS) and 10-m panchromatic (PAN) images (Welch and Ehlers, 1987; Carper *et al.*, 1990), and to combine Landsat image data with radar, air-borne geophysical, and thematic map information (Harris *et al.*, 1990). Carper *et al.* (1990) demonstrated that the intensity image from the forward IHS transformation of SPOT XS data can simply be replaced with high-resolution PAN data before performing the reverse IHS transformation. As a result, the output image retained the multispectral color (hue and saturation) information of the XS bands and gained the 10-m resolution of the PAN (intensity) image; a two-fold increase in resolution.

Unlike SPOT, however, where XS and PAN data are simultaneously recorded (co-registered) digital images (Carper *et al.*, 1990), the merger of dissimilar data (e.g., a digital Landsat image with an analog aerial photograph) requires several preprocessing steps before the IHS transformation merger can be performed. The benefit is that diverse forms of terrain information can be combined into a single hybrid data set to improve interpretation and mapping. Moreover, multi-band images with spectral and spatial properties comparable to SPOT can be produced from more readily available image data.

Study Site

The procedures presented in this paper were developed to improve identification and mapping of small, remnant landforms at the margins of a late-Quaternary paleolake, Lake Wamsutter, from available Landsat data and aerial photographs (Grasso, 1990). This lake, named for the town of Wamsutter, Wyoming, once occupied some 2,000 km² of the Great Divide Basin in the high desert area of south-central Wyoming (Figure 1); an area for which SPOT data was unavailable. At its maximum level of 2,040 to 2,045 m (6,693 to 6709 ft), the lake was about 67 to 72 m (220 to 236 ft) deep at Battle Springs Flat (1,973 m; 6,473 ft) and engulfed two subbasins: Red Desert Basin (RDB) to the west, and an east-trending valley now occupied by Lost Creek Basin (LCB), Battle Spring Flat (BSF), and Chain Lakes Flat (CLF). Today, remnant wave-cut shorelines, channel-mouth deltas, and lake-marginal sand dunes demarcate the former extent and littoral zone of the lake. From large-scale geologic interpretations of these paleolake landforms, it was possible to reconstruct the paleogeography of the lake and to ultimately decipher the late-Quaternary evolution of the basin.

Methods

Three available data sets were used to investigate small paleolake landforms at lake-marginal locations such as the Stratton Draw site (Figure 1). They were (1) Landsat Multispectral Scanner (MSS) and Thematic Mapper (TM) image data, (2) NASA high-altitude, color-infrared aerial photographs (1:100,000 scale), and (3) USGS 7½-minute topographic maps. Although Landsat image data furnished spectral information for differentiating surface sediment composition, they lacked essential spatial resolution for large-scale mapping (Figures 2a and 2b). Conversely, aerial photographs were indispensable for mapping paleolake features (Reeves, 1968), but lacked important multispectral information (Figure 2c). A merger of these data was therefore necessary so that both spectral (sediment composition) and spatial (topographic) information would be available in a single data set.

In the following sections, the IHS transformation merger of Landsat MSS and aerial photographic data for the Stratton Draw (delta) site is presented. The merger entails five-steps: (1) digital preprocessing, (2) geometric correction and co-registration, (3) forward IHS transformation, (4) reverse IHS transformation, and (5) display of hybrid image data.

Image processing was conducted on an 80386-based microcomputer workstation equipped with Map and Image Processing System (MIPS) software developed by Micro-Images, Inc., Howtek Scanmaster color flat-bed digitizing scanner, and high-resolution (1280 by 1024) color display system. Digital image data were prepared from nine-track Landsat MSS (ID 30104-17185; 06-17-78) and TM (ID 50127-17174; 07-06-84) computer-compatible tapes and a NASA color-infrared aerial photographic transparency (08-09-73).

Digital Preprocessing

The IHS transformation is a mathematical procedure that operates on digital, raster-based images. An analog aerial photograph (or map) must, therefore, be converted to a digital format compatible with Landsat by a process known as digitizing. To obtain maximum spatial information, the photograph should be digitized in panchromatic mode at the highest possible resolution (i.e., smallest pixel size) appropriate to its use. Two factors that constrain pixel size are (1) the resolution of the scanner, and (2) the scale of the photograph. A digitizing scanner with a maximum resolution of 300 dpi (dots per inch), for example, will produce a pixel size of 8.47 m from a 1:100,000-scale aerial photograph (i.e., 100,000 ÷ 300 = 333.33 inches or 8.47 m).

In the examples presented here, the maximum resolution of the scanner (300 dpi) was used to achieve the highest possible spatial resolution (8.47 m) from the aerial photograph. A pixel size adjustment to 10 m was subsequently made by

resampling the image during geometric correction and co-registration.

Geometric Correction and Co-Registration

In this second step of the merger, the digital Landsat bands and aerial photograph were geometrically corrected and co-registered to a common pixel size and map projection. A series of ground control points (GCPs) of known latitude and longitude were used to correct the images and remove distortion due to topographic irregularity and system inherent error (Friedmann *et al.*, 1983; Jensen, 1986). At the same time, the images were numerically resampled (Lillesand and Kiefer, 1987) to a common pixel size and rotated north. An even pixel size of 10 m was used to retain the maximum spatial resolution of the aerial photograph.

Figures 2a and 2b show the results applied to Landsat MSS and TM bands. In these cases, cubic convolution resampling was used to enlarge the images rather than simple pixel duplication because of the inherent ability of the algorithm to reduce (smooth) image blockiness (Jensen, 1986). Although the images still appeared blurred due to the required 8× (MSS) and 3× (TM) enlargements, this was of little consequence because only the spectral (hue and saturation) information was needed for the merger.

For the digitized aerial photograph, nearest neighbor resampling was used to adjust its pixel size from 8.47 m to 10.0 m and to rotate the image 17.63 degrees (counter-clockwise) to north. Figure 2c shows that the spatial integrity of the aerial photograph was maintained during these steps.

As a final preprocessing step, the geometrically corrected images were co-registered, using GCPs as reference, and trimmed to a common line and column (matrix) size. The accuracy of these steps was essential in that any error in geometric correction or co-registration would have resulted in a mismatch between spectral and spatial information during the IHS transformation merger.

Forward IHS Transformation

Using the forward (RGB to IHS) transformation, the standard false-color-infrared Landsat image (MSS-7 as red, MSS-5 as green, and MSS-4 as blue) was orthogonally transformed into its corresponding IHS components. As a result, the intensity component contained spatial information corresponding to surface morphology, while the hue and saturation components contained spectral information related to the average color of surface reflected light and its apparent brightness (or purity), respectively. Thus, the Landsat multispectral color information, as detected in the green to near-infrared spectral range of the MSS bands (0.50 to 0.60, 0.60 to 0.70, and 0.80 to 1.10 μm), was effectively separated by the forward transformation into hue and saturation components.

Reverse IHS Transformation

At this point of the merger the Landsat intensity component, which contained only lower resolution (80-m) MSS spatial information, was replaced by the higher resolution aerial photograph and the reverse IHS transformation was performed. As a result, the 10-m spatial information of the photograph

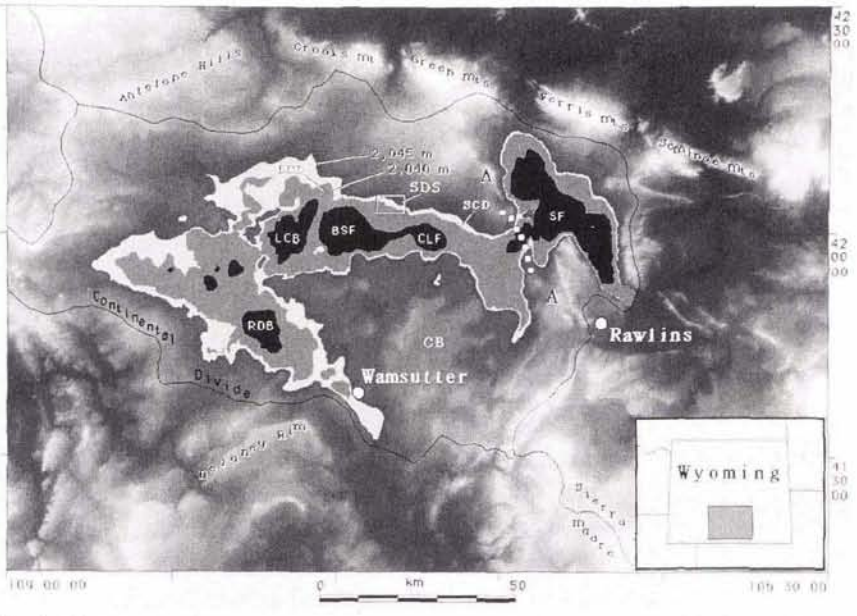

Fig. 1. Digital elevation model of the Great Divide Basin, Wyoming. The basin is internally drained and encircled by the Continental Divide. Five-metre elevation levels are displayed in 240 shades from dark gray (low) to light gray (high). Shown are the maximum extent of Lake Wamsutter at the 2,040- to 2,045-m level in white; the locations of three well preserved deltas at Lost Creek (LCD), Stewart Creek (SCD), and Stratton Draw (SDS); and the former site of basin closure (dotted line) west of Separation Flats (SF). Today, Separation Creek cuts near-vertical rocks of the west flank of the Rawlins uplift (A). Sites of Holocene (?) closed-basin pluvial lakes are shown in black (less than 2,010 m) in the deepest parts of the basin west of SF. (after Grasso, 1990)

was effectively combined with the spectral information of the Landsat hue and saturation components. This merger is particularly appropriate because the approximate spectral range of the color-infrared photograph (0.50 to 0.90 μm) is comparable to that of the Landsat bands (0.50 to 1.10 μm). Thus, very little spectral (color) modification occurs during the merger.

Display of Hybrid Image Data

Red, green, and blue output images from the preceding step could now be displayed as a color composite. The display was comparable to a standard false-color-infrared image because Landsat multispectral data were preserved during the IHS transformation merger. The most noticeable consequence, however, was that the 80-m resolution of the MSS scene (Figure 2a) was elevated to the 10-m resolution of the aerial photograph (Figure 2c); an eight-fold increase in topographic resolving power.

Results of the IHS Transformation Merger

Plate 1 shows that the IHS transformation merger is particularly well suited for combining image data with large differences in spatial resolution. At the Stratton Draw site, the improved resolution of the color hybrid image was particularly valuable for mapping small lake-marginal landforms. The image reveals, for example, that a well-preserved delta extends from the mouth of Stratton Draw onto the dry lake bed of Lake Wamsutter, whereas on the MSS scene of the site

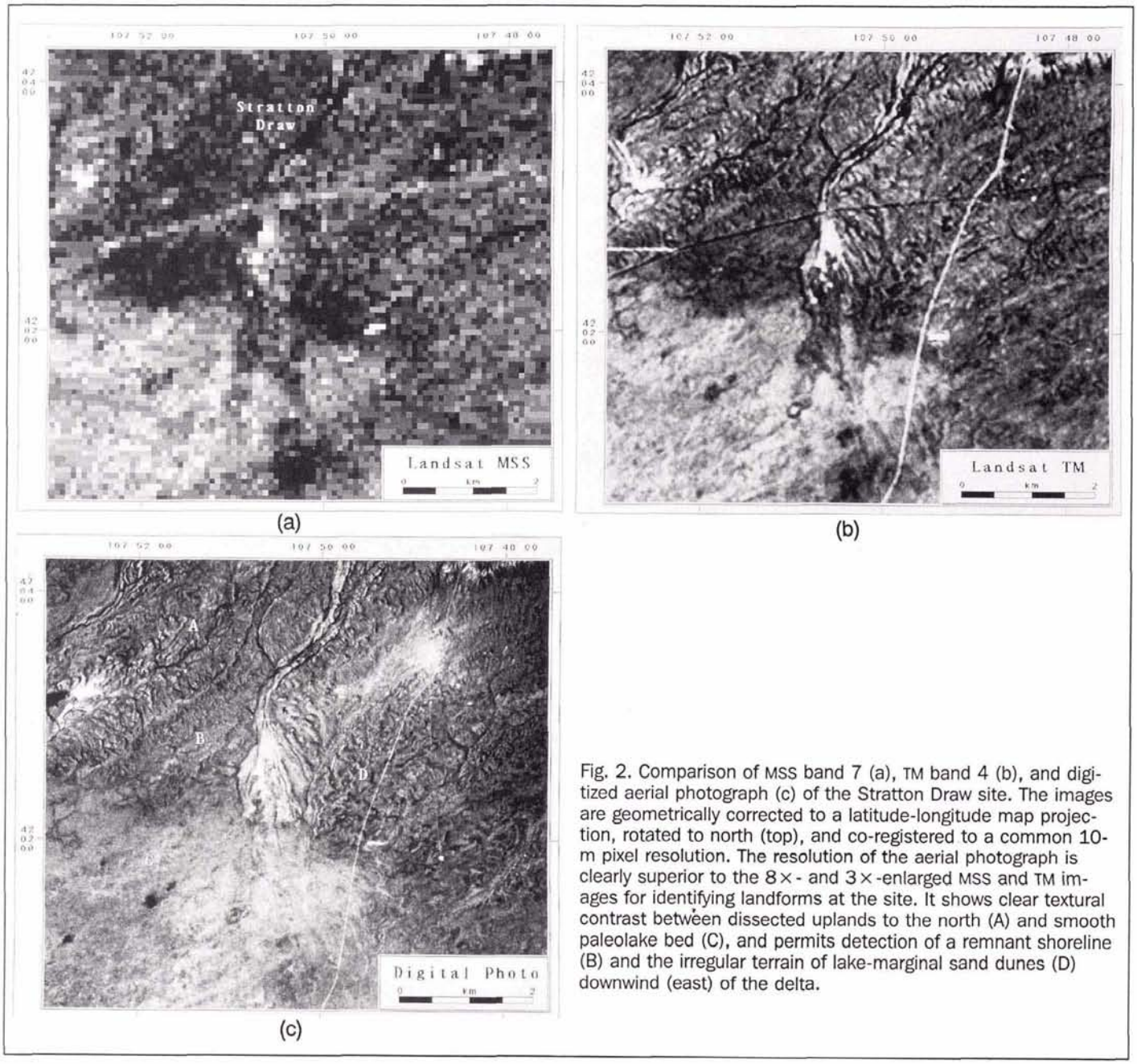

Fig. 2. Comparison of MSS band 7 (a), TM band 4 (b), and digitized aerial photograph (c) of the Stratton Draw site. The images are geometrically corrected to a latitude-longitude map projection, rotated to north (top), and co-registered to a common 10-m pixel resolution. The resolution of the aerial photograph is clearly superior to the 8× - and 3×-enlarged MSS and TM images for identifying landforms at the site. It shows clear textural contrast between dissected uplands to the north (A) and smooth paleolake bed (C), and permits detection of a remnant shoreline (B) and the irregular terrain of lake-marginal sand dunes (D) downwind (east) of the delta.

(Figure 2a) this feature could not be explicitly identified. The image more clearly shows the former maximum lake boundary due to textural differences between the dissected terrain to the north (A) and spectrally homogeneous lake bed (C), and reveals important geomorphic relationships between these features and remnant shoreline (B) and lake-marginal sand dunes (D). The spatial association between these landforms served to document their lacustrine origin.

Two additional attributes of the IHS-transformed RGB image components are (1) they are raster images, and (2) they are co-registered to the original Landsat bands. Thus, digital enhancements (e.g., edge-enhancement filtering) can be applied to improve discrimination of geologic landforms and structures, thematic map information can be added as a digital overlay to improve analysis, and co-registered Landsat bands can be used for spectral analysis or other digital interpretation and classification activities. For example, the superimposed 1:24,000-scale topographic map was particularly useful for morphometric analysis and mapping at the Stratton Draw site (Plate 1). These contour data effectively show the maximum lake level, that the delta is approximately 1.0 mile (1.6 km) long (north to south) and 0.75 mile (1.2 km) wide (east to west), and that it has an average slope of 0.45 degrees from its proximal to distal ends.

Thematic Applications of the IHS Transformation

An important disadvantage of the IHS transformation as an image merging tool is its apparent inability to combine spectrally dissimilar data. While the merger provides a significant improvement in overall interpretability, the narrow spectral coverage of the image (green to near-infrared) limits its use to general landscape interpretation or vegetation and agricultural applications. Goetz *et al.* (1983, p. 575), recognizing this limitation, noted that for geologic purposes the spectral coverage of Landsat MSS "does not extend into regions of the spectrum most useful in characterizing the spectral properties of geologic surface materials." The same can also be said of course for infrared photography and SPOT imagery because of their analogous spectral ranges.

For geologic remote sensing, the merger of short-wave infrared (SWIR) or thermal infrared spectral data and high-resolution spatial data would be particularly valuable. In the SWIR region, unique spectral reflectance and absorption features were shown by Hunt (1977, 1979) and Hunt and Ashley (1979) to be directly related to distinctive mineralogical properties. Within this region, most geologic materials exhibit reflectance maxima near 1.60 μm wavelength (Prost, 1980). A suite of phyllosilicate minerals (e.g., hydroxylated silicates such as clays) additionally has reflectance minima centered at 2.20 μm due to absorption bands in the 2.10- to 2.35-μm region caused by vibrational processes associated with the Al-O-H bond (Prost, 1980; Goetz, *et al.*, 1983). The sensitivity of this absorption feature was demonstrated by Hunt and Ashley (1979) who were able to detect hydroxyl absorption in rocks containing only 13 percent clay.

The presence of these spectral traits has led to the widespread use of the SWIR spectrum in geologic remote sensing (Rowan *et al.*, 1974; Abrams *et al.*, 1977, 1983; Goetz and Rowan, 1981; Lang *et al.*, 1984a, 1984b; Yamaguchi, 1987; Campos-Marquetti and Rockwell, 1989; Pontual, 1989). For example, Podwysocki and Segal (1983) used the 1.60/2.20-μm band ratio to detect the abundance of clays in geologic surface materials. They found that areas of intense 2.20-μm absorption were dominated by high concentrations of hydrothermally altered minerals (clays) associated with subsurface economic mineral deposits.

Spectral Detection of Sediments at Stratton Draw

At the Stratton Draw site, Landsat bands TM-5 (1.55 to 1.75 μm) and TM-7 (2.08 to 2.35 μm) and the TM-5/7 ratio (1.65/2.20 μm) were used to differentiate sediment types associated with paleolake landforms. In this lake-marginal area, eolian sand dunes contain very little clay and have low TM-5/7 values, whereas clay-rich fluvial-lacustrine and lacustrine landforms, such as the delta and lake bed (L-Bed(d)) at its terminus, have higher ratio values (Figure 3). These ratio spectra additionally showed that the shoreline (Shore) and nearshore (Lake Bed) contain only minor amounts of clay due to the winnowing action of waves that once dominated this higher-energy lake zone.

The problem was, however, that, while the TM ratio clearly revealed sediment composition of paleolake landforms at the site, the lower resolution of the enlarged TM image (Figure 2b) and noise generated by the ratio yielded inadequate spatial resolution for accurate large-scale mapping. Thus, a merger of the TM-5/7 ratio image and the digitized aerial photograph was necessary.

IHS Transformation Merger of Mixed Spectra Data

Two techniques, both using the reverse IHS transformation, were found to be appropriate for merging these mixed-spectra data even though the spectral content of Landsat TM-5 and TM-7 bands was only weakly correlated with that of the digitized aerial photograph (correlation coefficients of 0.335 and 0.355, respectively). The methods are similar in that only two variables, intensity and hue or intensity and saturation, are used to produce high-resolution "colorized" displays. In both, base (spatial) information is supplied by the intensity component (e.g., a co-registered digitized aerial photograph), while color (thematic) information is provided by either hue or saturation, which is added to the base as a type of thematic overlay by the reverse IHS transformation.

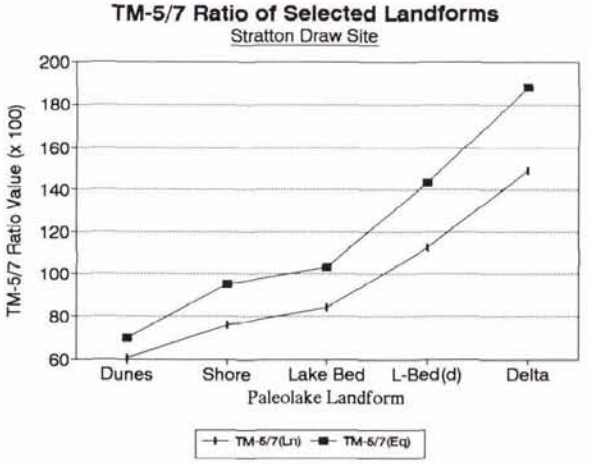

Fig. 3. TM-5/7 ratio spectra of select paleolake landforms. Higher ratio values correspond to increasing concentrations of clay. Delta deposits contain the greatest amounts of clay, while eolian sand dunes contain the least. Clay-rich fluvial deposits (Delta) were derived from weathered Tertiary bedrock in the north and transported to the lake margin by Stratton Draw. Higher concentrations of clay in lake bed deposits at the toe of the delta (L-Bed(d)) are the result of this influx. (Contrast stretches: Ln = linear; Eq = equalize)

An important advantage of these techniques is that color interpretation is limited to a single variable.

In the first approach, hue is used as the dominant thematic component and saturation is held at a constant value. The reverse IHS transformation, therefore, adds color to the base (intensity) image in response to the information content of hue. Using this technique, Harris *et al.* (1990) showed that diverse forms of satellite image data and map information can be successfully integrated. The problem is, however, that large variations in hue can generate broad color spectra differences that may be difficult to interpret from the resulting RGB output display.

In the second approach, saturation is used as the dominant thematic component and hue is held at a constant value. The advantage of this approach is that an individual color (hue) can be used for the thematic overlay. Variations in color purity (saturation) will, therefore, systematically change within the range of the single hue value in response to the information content of the saturation component (Yamaguchi, 1987). For example, if a TM-5/7 ratio image is used as the saturation component, areas of higher clay content as detected by higher TM-5/7 values will be exhibited by purer or more vivid (i.e., more saturated) colors. Conversely, areas of lower clay concentrations would be shown in pale (pastel) or unsaturated colors.

Results of the Mixed Spectra Merger

Plate 2 shows the results achieved at the Stratton Draw site using the second of the above approaches. This thematic image map of sediment composition at the site was prepared using a digitized, 10-m resolution NASA aerial photograph as intensity and a 9 by 9 low-pass-filtered TM-5/7(Eq) ratio image as saturation. Hue, the third IHS component, was furnished by a neutral gray level image with pixel values of 96 (0 to 255 scale). These IHS components were subsequently combined using the reverse IHS transformation, and the resulting RGB image components were displayed.

As Plate 2 illustrates, low-to-high clay concentrations detected by the TM-5/7 ratio are systematically portrayed in shades of yellow-orange to deep-red over the full saturation range of hue equal 96. In areas where sediments are exceptionally clay poor, low TM-5/7 values produced poorly saturated colors in shades of gray-blue to gray-green depending on the intensity value for the area. The sand dune field, east (downwind) of the delta, is one such area where clay-poor (silica-rich) sands dominate. Here, TM-5/7 values of 60 to 70 and intensity values of 125 to 150 produced poorly saturated gray-blue colors, whereas lower intensity values of about 75 in the interdunal areas generated gray-green colors.

An important result of the merger is that the TM-5/7 ratio furnished lithologic information as a single-variable color overlay for the high-resolution aerial photograph. Paleolake landforms at the site could therefore be interpreted and mapped on the basis of both sediment composition, as revealed by the TM-5/7 ratio (Figure 3), and morphometric information supplied by the high-resolution aerial photograph (Figure 2c). Furthermore, geologic analysis was simplified by the single-variable color information and its direct correspondence to color purity.

In preparing these images, it was found that different values of hue can be used to produce image maps in any desired color gradation (blue, green, purple, etc.). A hue of 64, for example, would have exhibited changes in clay content at the Stratton Draw site in systematically changing shades of lavender to purple.

Plate 1. False-color-infrared "hybrid" image map of the Stratton Draw site. Its 10-m resolution is governed by the digitized aerial photograph (intensity). Color information (hue and saturation) is comparable to a Landsat MSS 7-5-4 (R-G-B) display. Shown are rough dissected terrain above the maximum level of the lake (A); remnant shoreline (B); spectrally homogeneous paleolake bed (C); and lake-marginal sand dunes (D) downwind of the delta. Heavier growths of sagebrush and grasses are revealed by red mottling. The triangular morphology of the delta and location of slope measurement sites (A to B) are show on the 2×-enlarged (5-m pixel size) inset map.

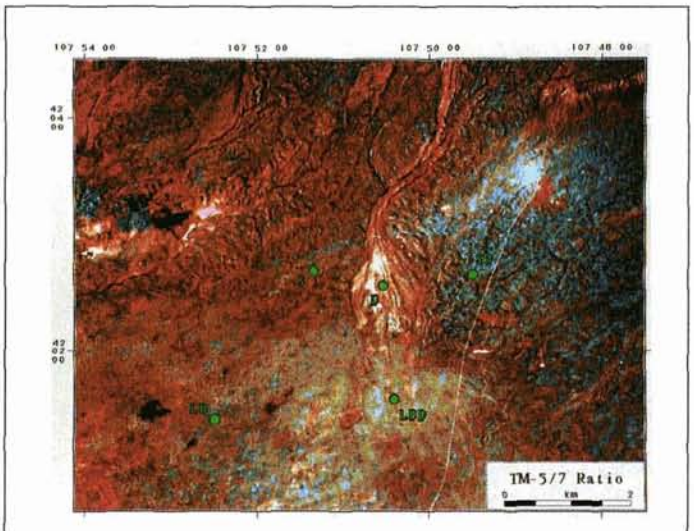

Plate 2. Reverse IHS transformation merger of digitized, 10-m resolution aerial photograph (intensity), TM-5/7(Eq) ratio (saturation), and neutral gray level image (hue). A 9 by 9 low-pass filter was applied to the ratio image before the merger to reduce ratio-generated noise and image complexity. Low to high clay concentrations are shown in shades of yellow-orange to deep-red, respectively. TM-5/7 values for select paleolake landforms (green circles) are given in Figure 3. (D = Delta; SD = Sand Dunes (Dunes); LB = Lake Bed; LBD = Lake Bed at Delta toe (L-Bed(d)); S = Shoreline (Shore))

Conclusion

The IHS transformation is a useful and powerful tool for combining remotely sensed image data having large (8×) differences in spatial resolution, while other merging techniques (e.g., band replacement) are restricted to smaller (2× to 3×) differences. Its application permits readily available Landsat (MSS or TM) multi-band imagery and high-altitude aerial photography to be merged into single hybrid data sets having spectral (green to near-infrared) and spatial (10 m) properties comparable to SPOT imagery. An important benefit of this approach is that these high-resolution multispectral images can be produced for study sites where more advanced satellite data, such as SPOT, are unavailable or when their higher costs are prohibitive.

Although the IHS transformation merger is best suited for remotely sensed data having similar spectral coverage (e.g., Landsat MSS bands 4, 5, and 7 or TM bands 2, 3, and 4 with color-infrared aerial photographs), short-wave infrared, thermal infrared, band ratios, and multispectral indices or classifications can be integrated with the information content of a digitized aerial photograph through the application of two alternative methods. These mixed spectra mergers, both employing only the reverse IHS transformation, are particularly important to geologic remote sensing because they allow diverse forms of spectral and spatial landscape information to be combined into a single data set for analysis. The spatial distribution of exposed rock, sediment, or soil can, therefore, be examined in conjunction with other forms of pertinent morphologic or thematic data that may be available from such sources as aerial photographs, radar images, digital elevation and slope models, and thematic maps. Through the application of these techniques, digital and analog terrain data can be combined to prepare two- and three-dimensional thematic image models of the Earth that show complex relationships in more easily interpretable formats.

Acknowledgment

Funding and laboratory facilities for this investigation were provided by the Department of Geology and Geophysics, University of Wyoming. Special thanks are due to Professor Ronald Marrs for his technical assistance, and to Karen Kempton for her gracious support and constructive critiques of the manuscript.

References

Abrams, M. J., R. P. Ashley, I. C. Rowan, A. F. H. Goetz, and A. B. Kahle, 1977. Mapping of Hydrothermal Alteration in the Cuprite Mining District, Nevada, Using Aircraft Scanner Images for the Spectral Region 460 to 2360 nm, *Geology*, Vol. 5, pp. 713-718.

Abrams, M. J. D. Brown, L. Lepley, and R. Sadowski, 1983. Remote Sensing for Copper Exploration in Southern Arizona, *Economic Geology*, Vol. 78, pp. 591-604.

Avery, T. E., and G. L. Berlin, 1985. *Interpretation of Aerial Photographs*, Fourth Edition, Burgess Publishing Co., 554 p.

Buchanan, M. D., and R. Pendergrass, 1980. Digital Image Processing: Can Intensity, Hue, and Saturation Replace Red, Green, and Blue?, *Electro-Optical Systems Design*, (EOSD), March, 1980.

Campos-Marquetti, R., Jr., and B. Rockwell, 1989. Quantitative Lithologic Mapping in Spectral Ratio Feature Space: Volcanic, Sedimentary and Metamorphic Terrains, *Proceedings of the 7th Thematic Conference on Remote Sensing for Exploration Geology*, Calgary, Alberta, pp. 471-484.

Carper W. J., T. M. Lillesand, and R. W. Kiefer, 1990. The Use of Intensity-Hue-Saturation Transformations for Merging SPOT Panchromatic and Multispectral Image Data, *Photogrammetric Engineering & Remote Sensing*, Vol. 56, No. 4, pp. 459-467.

Chavez, P. S., Jr., 1986, Digital Merging of Landsat TM and Digitized NHAP Data for 1:24,000-Scale Image Mapping, *Photogrammetric Engineering &d Remote Sensing*, Vol. 52, No. 10, pp. 1637-1646.

Chavez, P. S., Jr., G. L. Berlin, and L. B. Sowers, 1982. Statistical Methods for Selecting Landsat MSS Ratios, *Applied Photographic Engineering*, Vol. 8, No. 1, pp. 23-30.

Chavez, P. S., Jr., and J. A. Bowell, 1988. Comparison of the Spectral Information Content of Landsat Thematic Mapper and SPOT for Three Different Sites in the Phoenix, Arizona, Region, *Photogrammetric Engineering & Remote Sensing*, Vol. 54, No. 12, pp. 1699-1708.

Chavez, P. S., Jr., S. C. Guptill, and J. Bowell, 1984. Image Processing Techniques for Thematic Mapper Data, *Proceedings: 50th Annual ASP-ACSM Symposium*, American Society of Photogrammetry, Washington, D.C., pp. 728-743.

Cliche, G., F. Bonn, and P. Teillet, 1985. Integration of the SPOT Panchromatic Channel into Its Multispectral Mode for Image Sharpness Enhancement, *Photogrammetric Engineering & Remote Sensing*, Vol. 51, No. 3, pp. 311-316.

Daily, M., 1983. Hue-Saturation-Intensity Split-Spectrum Processing of Seasat Radar Imagery, *Photogrammetric Engineering & Remote Sensing*, Vol. 49, No. 3, pp. 349-355.

Drury, S.A., 1987. *Image Interpretation in Geology*, Allen and Unwin, London, 243 p.

Friedmann, D. E., J. P. Friedel, K. L. Magnussen, R. Kwok, and S. Richardson, 1983. Multiple Scene Precision Rectification of Spaceborne Imagery with Very Few Ground Control Points, *Photogrammetric Engineering & Remote Sensing*, Vol. 49, pp. 1657-1667.

Gillespie, A. R., 1980. Digital Techniques of Image Enhancement, *Remote Sensing in Geology* (B. S. Siegal and A. R. Gillespie, editors), John Wiley and Sons, New York, pp. 139-226.

Gillespie, A. R., A. B. Kahle, and R. E. Walker, 1986. Color Enhancement of Highly Correlated Images. I. Decorrelation and HSI Contrast Stretches, *Remote Sensing of Environment*. Vol. 20, pp. 209-235.

Goetz, A. F. H., and L. C. Rowan, 1981, Geologic Remote Sensing, *Science*, Vol. 211, pp. 781-791.

Goetz, A. F. H., B. N. Rock, and L. C. Rowan, 1983. Remote Sensing for Exploration: An Overview, *Economic Geology*, Vol. 78, No. 4, pp. 573-590.

Grasso, D., 1990. *Recognition and Paleogeography of Quaternary Lake Wamsutter (A Proposed Lake in Wyoming's Great Divide Basin) Combining Landsat Remote Sensing and Digital Elevation Modeling*, Unpublished Ph.D. Dissertation, Department of Geology and Geophysics, University of Wyoming, 184 p.

Harris, J. R., R. Murray, and T. Hirose, 1990. IHS Transformation for the Integration of Radar Imagery with Other Remotely Sensed Data, *Photogrammetric Engineering & Remote Sensing*, Vol. 56, No. 12, pp. 1631-1641.

Haydn, R., and others, 1982. Application of the IHS Color Transformation to the Processing of Multisensor Data and Image Enhancement, *Proceedings of the International Symposium on Remote Sensing of Arid and Semiarid Lands*, Cairo, Egypt, pp. 599-616.

Hunt, G. R., 1977. Spectral Signatures of Particulate Minerals in the Visible and Near Infrared, *Geophysics*, Vol. 42, pp. 501-513.

———, 1979. Near Infrared (1300-2400 nm) Spectra of Alteration Minerals - Potential for Use in Remote Sensing, Geophysics, Vol. 44, 1974-1986.

Hunt, G. R., and R. P. Ashley, 1979. Spectra of Altered Rocks in the Visible and Near Infrared, *Economic Geology*, Vol. 74, pp. 1613-1629.

King, R. W., V. H. Kaupp, W. P. Waite, and H. C. MacDonald, 1984. Digital Colour Space Transformations, *Proceedings of IGARSS '84 Symposium*, Strasbourg, August, pp. 649-654.

Jensen, J. R., 1986. *Introductory Digital Image Processing: A Remote Sensing Perspective*, Prentice-Hall, Englewood Cliffs, New Jersey. 379 p.

Judd, D. B., and G. Wyszecki, 1975. *Color in Business, Science and Industry*, 3rd ed., John Wiley and Sons, New York.

Kahle, A. B., 1980a. Middle Infrared MSS Aircraft Scanner Data:

Analysis for Geologic Applications, *Applied Optics*, Vol. 19, pp. 2279-2290.

———, 1980b. Surface Thermal Properties, *Remote Sensing in Geology* (B. S. Siegal and A. R. Gillespie, editors). John Wiley and Sons, New York, pp. 257-273.

Lang, H. R., W. H. Alderman, and F. F. Sabins, Jr., 1984a. Patrick Draw, Wyoming, Petroleum Test Case Report, Section 11, *The Joint NASA/Geosat Test Case Project: Final Report* (M. J. Abrams, J. E. Conel, and H. R. Lang, editors), Part 2, Volume II, pp. 11-1 to 11-112.

Lang, H. R., S. M. Nicolais, and H. R. Hopkins, 1984b. Coyanosa, Texas, Petroleum Test Site Report, Section 13, *The Joint NASA/Geosat Test Case Project: Final Report* (M. J. Abrams, J. E. Conel, and H. R. Lang, editors), Part 2, Volume II, pp. 13-1 to 13-81.

Lillesand, T. M., and R. W. Kiefer, 1987. *Remote Sensing and Image Interpretation*, 2nd ed., John Wiley and Sons, New York, 708 p.

Moik, J.G., 1980. *Digital Processing of Remotely Sensed Images.* NASA Special Publication. SP-431, 330 p.

Podwysocki, M. H., and D. B. Segal, 1983. Use of Multispectral Scanner Images for Assessment of Hydrothermal Alteration in the Marysvale, Utah, Mining Area, *Economic Geology*, Vol. 78, pp. 675-687.

Pontual, A., 1989. Lithological Information in Enhanced Landsat Thematic Mapper Images of Arid Regions, *Proceedings of the 7th Thematic Conference on Remote Sensing for Exploration Geology*, Calgary, Alberta, pp. 379-393.

Prost, G., 1980. Alteration Mapping with Airborne Multispectral Scanners, *Economic Geology*, Vol. 75, pp. 894-906.

Reeves, C. C., Jr., 1968. *Introduction to Paleolimnology*, Developments in Sedimentology 11, Elsevier Publishing Company, Amsterdam, London, New York, 228 p.

Robertson, P. K., and J. F. O'Callaghan, 1988. The Application of Perceptual Color Spaces to the Display of Remotely Sensed Imagery, *IEEE Transactions on Geoscience and Remote Sensing*, Vol. 26, No. 1, pp. 49-59.

Rowan, L. C., P. H. Wetlaufer, A. F. H. Goetz, F. C. Billingsley, and J. C. Stewart, 1974. *Discrimination of Rock Types and Detection of Hydrothermally Altered Areas in South-Central Nevada by the Use of Computer-Enhanced ERTS Images*, U. S. Geological Survey Profession Paper, No. 883, 35 p. Rowan, L. C., P. H. Wetlaufer, A. F. H. Goetz, F. C. Billingsley, and J. H. Stewart, 1983. Discrimination of Rock Types and Detection of Hydrothermally Altered Areas in Southcentral Nevada by Use of Computer Enhanced ERTS Images, *Remote Sensing* (K. Watson and R. D. Regan, editors), Geophysics Reprint Series, No. 3, pp. 23-57.

Shih, E. H. H., and R. A. Schowengerdt, 1983. Classification of Arid Geomorphic Surfaces Using Landsat Spectral and Textural Features, *Photogrammetric Engineering & Remote Sensing*, Vol. 49, No. 3, pp. 337-347.

Siegal, B. S., and A. R. Gillespie, 1980. *Remote Sensing in Geology*, John Wiley and Sons, New York, 536 p.

Welch, R., and M. Ehlers, 1987. Merging Multiresolution SPOT HRV and Landsat TM Data, *Photogrammetric Engineering & Remote Sensing*, Vol. 53, No. 3, pp. 301-303.

Yamaguchi, Y., 1987. Possible Techniques for Lithologic Discrimination using the Short-Wavelength-Infrared Bands of the Japanese ERS-1, *Remote Sensing of Environment*, Vol. 23, pp. 117-129.

(Received 30 July 1991; accepted 16 March 1992; revised 3 June 1992)

FORTHCOMING ARTICLES

Richard Aspinall and *Neil Veitch*, Habitat Mapping from Satellite Imagery and Wildlife Survey Data Using a Bayesian Modeling Procedure in a GIS.

Deborah Burgess, Automatic Ship Detection in Satellite Multispectral Imagery.

Russell G. Congalton, Kass Green, and *John Teply*, Mapping Old Growth Forests on National Forest and Park Lands in the Pacific Northwest from Remotely Sensed Data.

Russell G. Congalton and *Kass Green*, A Practical Look at the Sources of Confusion in Error Matrix Generation.

John R. Dymond, An Improved Skidmore/Turner Classifier.

Maria Fiorella and *William J. Ripple*, Determining Successional Stage of Temperate Coniferous Forests with Landsat Satellite Data.

Douglas G. Goodin, Luoheng Han, Rolland N. Fraser, Donald C. Rundquist, and *Wesley A. Stebbins*, Analysis of Suspended Solids in Water Using Remotely Sensed High Resolution Derivative Spectra.

Edwin J. Green, William E. Strawderman, and *Teuvo M. Airola*, Assessing Classification Probabilities for Thematic Maps.

John R. Jensen, Sunil Narumalani, Oliver Weatherbee, and *Halkard E. Mackey, Jr.*, Measurement of Seasonal and Yearly Cattail and Waterlily Changes Using Multidate SPOT Panchromatic Data.

D. Klimes and *D. I. Ross*, A Continuous Process for the Development of Kodak Aerochrome Infrared Film 2443 as a Negative.

Chris L. Lauver and *Jerry L. Whistler*, A Hierarchical Classification of Landsat TM Imagery to Identify Natural Grassland Areas and Rare Species Habitat.

Ann L. Maclean, Thomas P. D'Avello, and *Stephen G. Shetron*, The Use of Variability Diagrams to Improve the Interpretation of Digital Soil Maps in a GIS.

Oğuz Müftüoğlu, A Data Reduction Approach Using the Collinearity Model from Non-Metric Photography.

Tod D. Rubin, Spectral Mapping with Imaging Spectrometers.

Scott A. Samson, Two Indices to Characterize Temporal Patterns in the Spectral Response of Vegetation.

I. Tannous and *B. Pikeroen*, Parametric Modeling of Spaceborne SAR Image Geometry Application: SEASAT/SPOT Image Registration.

Gregory S. Tudor and *Larry J. Subarbaker*, GIS Orthographic Digitizing of Aerial Photographs by Terrain Modeling.

E. Wayne Vickers, Production Procedures for an Oversize Satellite Image Map.

Yong-Jian Zheng, Digital Photogrammetric Inversion: Theory and Application to Surface Reconstruction.